Analyzing additional wind effects to better optimize high-rise structural design

by

Benjamin L. VanNierop

B.S., Kansas State University, 2025

A REPORT

submitted in partial fulfillment of the requirements for the degree

MASTER OF SCIENCE

G.E. Johnson Department of Architectural Engineering and Construction Science

Carl R. Ice College of Engineering

KANSAS STATE UNIVERSITY
Manhattan, Kansas

2026

Approved by:

Major Professor
Kyle H. Larson, PhD., P.E.

Copyright

Abstract

The current ASCE 7-22 provides a comprehensive framework for determining the baseline wind forces on high-rise structures for static pressures. However, it overlooks dynamic wind effects such as vortex shedding and dynamic amplification. This report aims to address the additional wind effects not specified in ASCE 7-22. Through calculations for both static and dynamic winds, a comparison was made showing that the addition of dynamic wind loads not considered in ASCE 7-22 altered the overall wind load and modified the base shear and sidewall force from static pressures. Due to this, suggested design considerations for high-rise buildings were developed to better match the new base shear and adjusted sidewall forces with all wind effects in consideration.

To show how these new design considerations can be applied, a steel-framed structure located in Miami, Florida, will be analyzed. The structure will have a 120 ft x 120 ft footprint with a height of 480 ft. This case study will be used to determine the wind forces along the structure as defined in ASCE 7-22, as well as to determine any changes in base shear and sidewall forces additional wind effects applies to the structure.

Table of Contents

List of Figures

List of Tables

Chapter 1: Introduction

Structural engineers' emphasis is on both optimization and occupant safety when designing a building's structure. To achieve this, engineers must consider multiple different load characteristics acting along the building's faces. Among these, environmental loads are particularly important due to their unique characteristics and continual changes throughout different projects. A main aspect of these environmental loads comes from the force exerted by wind. Wind loading is a unique property because the forces acting on a structure depend on several factors, including wind speed, building shape and height, as well as terrain and location. These properties create different loads along the building's structure such as uplift, lateral, and shear. Shear loading is often a governing design consideration due to its significant influence on structural performance and failure modes.

This report addresses additional wind effects that high-rise infrastructures may experience beyond those directly addressed in the ASCE 7-22 (American Society of Civil Engineers, 2022). The building codes stated in ASCE 7-22 regarding high-rise lateral wind do address the total loading the building will experience at each elevation. However, it does not fully address additional aerodynamic properties high-rise structures may experience such as vortex shedding and dynamic amplification. By analyzing these additional effects, the goal is to better optimize the overall structural design of high-rises. With a more refined loading diagram, it may be necessary to modify the necessary structural steel sizes on any lateral bracing section within the building as well as adjust the cost of construction while still maintaining occupancy safety.

To compare the pre-existing wind load analysis to the additional lateral wind effect, a general high-rise structure will be used as a reference, and apply all wind loading equations will be applied. The structure will be made with the assumption that it will serve as a general-use office building with a default soil class (site class D per ASCE 7-22) and a risk category II classification. The location of the reference building will be Miami, Florida. Florida represents the urban environment with the third-highest number of high-rise structures in the United States with New York City and Chicago ranking first and second respectively (Chepkemoi, 2025). The decision of which city to choose came down to the maximum wind speed. Choosing Miami resulted in a wind speed of 170 mph which would result in a larger lateral wind force.

This case study structure will have the dimensions set at 120 ft x 120 ft with a height of 480 ft. Setting the base and width to be the same will simplify some calculations when determining base shear, and having the height at 480 ft is well above the classification of high-rise as stated in the International Building Code (International Code Council, 2024). There will be no parapet, and the roof will be considered flat with a slope of less than 15 degrees. The velocity pressure will be calculated every 20 ft to get the most accurate base shear calculation. The structural frame will be a main wind force resisting system (MWFRS) with a damping ratio of 1.5%, which will fall within the standard for most steel frame structures.

Chapter 2 of this report will focus on addressing the current wind equations outlined in ASCE 7-22 and break down the importance of each part and why it is necessary to include, specifically on high-rise structures, to understand the total lateral loading as well as the uplift on the roof design. To get the best understanding of how wind will interact with high-rise design the code equations will be applied to the high-rise case study to determine the total base shear for the building.

The next section, Chapter 3, will be a detailed analysis of additional wind effects to determine how they would apply to the high-rise case study. Each additional wind effect will be applied to the case study to determine the additional loading that the structure will experience and compare to the results from ASCE 7-22. The objective of this section is to assess how these effects could alter the wind loading distribution and overall structural design of the specified case study.

The last portion of this report will act as a design guide recommendation and conclusion. The focus will be to create design guide flowcharts for each additional wind effect to simplify the design process and make it easier to apply to future design projects. These additional wind effects will help address any changes ASCE should consider for future iterations of the wind code.

Chapter 2: ASCE 7-22 Analysis

2.0 ASCE Overview

The American Society of Civil Engineers (ASCE 2022) Standard 7, Minimum Design Loads and Associated Criteria for Buildings and Other Structures, is used by many engineers for building construction and design across federal, state, and local jurisdictions. The International Building Code (IBC 2024) adopted this code to be the primary U.S. standard governing the loads that structural systems must resist using minimum reliability and performance thresholds. The ASCE standard 7-22 covers dead, live, soil, flood, tsunami, snow, rain, ice, earthquake, and wind loads. Over the past decade, the ASCE has seen many changes especially within the wind loading chapters. Before the major changes in how the wind codes were adapted/written in 2010, the ASCE 7-05 wind chapters relied on a single set of basic wind speed maps based on the fastest mile wind statistics. In 2010, with the ASCE 7-10, the standard transitioned from fastest-mile speeds to 3-second gust basic wind speeds. The wind speed maps were recalibrated with the new 3-second gust speed, allowing load combinations to use a load factor of 1.0 for wind. ASCE 7-16 expanded on the 7-10 framework and introduced new aerodynamic research in the form of ground elevation factors, more detailed roof zone definitions, updated pressure coefficients for cladding/parapets/rooftop equipment/and solar panels, as well as revised topographic factors based on imposed modeling of speed effects. Finally, with the adoption of the ASCE 7-22, the wind maps were simplified with the use of the ASCE 7 hazard tool, now serving as the authoritative source for location-specific wind speed. ASCE 7-22 also had updates, including clarification to exposure assessments, expanded component and cladding pressure coefficients, better integration of simplified main wind force resisting systems (MWFRS) procedures for low-rise, and reorganization of the wind chapters to improve usability.

2.1 ASCE 7-22 Wind Equations

The ASCE 7-22 is the industry standard that addresses the wind loading on structural framing. These provisions provide a well-defined framework for calculating the lateral forces applied to all sides of a structure as well as the uplift force on the roof. To better understand how addressing additional wind effects may affect the building design, a design calculation needs to be conducted on the structural case study to understand how the standard codes summarize the total building shear at the base. To determine the windward and leeward forces on the project building, the use of equations from Chapters 26 & 27 within the ASCE 7-22 will be utilized. Chapter 26 (Wind loads: General Requirements) will address the velocity pressure at each 20 ft elevation, as well as determining the structure's exposure classification and wind factor effects for future calculations. Chapter 27 (Wind Loads on Building: Main Wind Force Resisting System) will be utilized to determine the wind pressure on each face of the building and used to calculate the base shear. By determining the base shear, it will be convenient to reference when comparing it to additional effects. In addition, the base shear comparison will be most optimal when looking at modifications to the overall structural steel. With that, the first set of calculations that will be computed comes from Chapter 26, the velocity pressure, q_z, shall be determined from:

$$q_z = 0.00256 K_z K_{zt} K_e V^2 \ (\mathrm{lb/ft^2}); V, \mathrm{mi/h} \tag{1}$$

Where;

K_z: Velocity pressure exposure coefficient

K_{zt}: Topographic factor

K_e: Ground elevations factor

V: Basic wind speed

q_z: Velocity pressure at height z (intervals of 20 ft)

The following factors: $K_z, K_{zt},$ & K_e can be determined from tables in Chapter 26. The ground elevation factor, K_e, shall be determined in multiple ways. The first is through the equation:

$$K_e = e^{-0.0000362 Z_e} \tag{2}$$

Where;

Z_e: Ground elevation above sea level

The second way to determine ground elevation factor is through *Table 26.9-1*, through which ASCE 7-22 makes a note that a conservative approximation is permitted so that $K_e = 1.0$ for all elevations. Due to this statement, along with the elevation of Miami only 6 ft above sea level (limit of 1,000 ft), the conservative factor will be used in the velocity pressure equation. Another factor listed in ASCE 7-22 is within the topographic factor; in order to simplify the velocity pressure equation a factor of $K_{zt} = 1.0$ can be used to achieve the highest-pressure value. The final table that will be used to calculate the total velocity pressure will be *26.10-1*, it will be assumed that the project building will be classified as exposure C. Since the velocity will be calculated at elevations of every 20 ft, the K_z coefficient can be taken from the table up to 480 ft. The K_z coefficient will need to be calculated for the remaining elevations using the following Equation:

$$K_z = 2.41\left(z/z_g\right)^{2/\alpha} \tag{3}$$

Where;

Z: Height above ground level

z_g: 2,460 ft (table 26.11-1 & Exposure C)

A: 9.8 (table 26.11-1 & Exposure C)

With the factors determined, the velocity pressure can be calculated at intervals of 20 ft using equation 1. The breakdown of the results is as follows:

Table 1: *Velocity Pressure at 20 ft Elevations*

Level (ft)	K_z	q_z (psf)
0	0.85	62
20	0.90	67
40	1.04	77
60	1.13	84
80	1.20	89
100	1.25	93
120	1.30	96
	….	
400	1.66	123
420	1.68	124
440	1.70	125
460	1.71	126
480	1.73	128

Before continuing to Chapter 27 to calculate the wind loads for the main wind resisting system (MWFRS), the building's natural frequency will be determined to understand the gust effect factor that will be applied to all sides of the high-rise. If the building can be assumed to be comprised of structural steel moment-resisting frames, the fundamental frequency equation can be taken as:

$$n_1 = \frac{22.2}{h^{0.8}} \tag{4}$$

Where;

h: Is representative of the total structure height (480 ft)

The approximate frequency can be calculated as 0.158 Hz, which is less than 1.0, resulting in ASCE 7-22 classifying the high-rise case study structure as a flexible structure. Due to this, ASCE 7-22 has a series of equations needed to determine the gust factor effect for a flexible building. If a simplified approach is to be used, then a gust factor effect of 0.85 can be taken. Unfortunately, the use of 0.85 is more suitable for a rigid structure, and the true gust factor may be larger resulting in a high base shear. The following equations will be necessary to determine the specific gust factor for this structure.

$$G_f = 0.925\left(\frac{1 + 1.7I_{\bar{z}}\sqrt{g_Q^2Q^2 + g_R^2R^2}}{1 + 1.7g_vI_{\bar{z}}}\right) \tag{5}$$

The background peak factors (g_Q and g_v) shall be taken as 3.4, with the resonant peak factor being calculated through the equation:

$$g_R = \sqrt{2\ln(3600n_1)} + \frac{0.577}{\sqrt{2\ln(3600n_1)}} \tag{6}$$

The background response factor, Q, intensity of turbulence at height z, $I_{\bar{z}}$, and resonant response factor, R¸ equations are as follows.

$$Q = \sqrt{\frac{1}{1 + 0.63\left(\frac{B + h}{L_{\bar{z}}}\right)^{0.63}}} \tag{7}$$

$$I_{\bar{z}} = c\left(\frac{33}{\bar{z}}\right)^{1/6} \tag{8}$$

$$R = \sqrt{\frac{1}{\beta} R_n R_h R_B (0.53 + 0.47 R_L)} \tag{9}$$

Where:

$$R_n = \frac{7.47 N_1}{(1 + 10.3 N_1)^{5/3}} \tag{10}$$

$$N_1 = \frac{n_1 L_{\bar{z}}}{\bar{V}_{\bar{z}}} \tag{11}$$

$$L_{\bar{z}} = l\left(\frac{\bar{z}}{33}\right)^{\bar{\varepsilon}} \tag{12}$$

$$\bar{V}_{\bar{z}} = \bar{b}\left(\frac{\bar{z}}{33}\right)^{\bar{\alpha}}\left(\frac{88}{60}\right)V \tag{13}$$

The size effect factors are related to the height (R_h), base (R_B), and depth (R_L) of the structure. Each size effect factor is based on turbulent coherence (correlation) factors in the corresponding directions, evaluated at the natural reduced frequency. The equation's breakdown is as follows:

$$R_h = \frac{1}{\eta_h} - \frac{1}{2\eta_h^2}\left(1 - e^{-2\eta_h}\right) \tag{14}$$

$$R_B = \frac{1}{\eta_B} - \frac{1}{2\eta_B^2}\left(1 - e^{-2\eta_B}\right) \tag{15}$$

$$R_L = \frac{1}{\eta_L} - \frac{1}{2\eta_L^2}\left(1 - e^{-2\eta_L}\right) \tag{16}$$

$$\eta_h = 4.6n_1\, h/\bar{V}_{\bar{z}} \tag{17}$$

$$\eta_B = 4.6n_1\, B/\bar{V}_{\bar{z}} \tag{18}$$

$$\eta_L = 15.4n_1\, L/\bar{V}_{\bar{z}} \tag{19}$$

Where

c: 0.20 (*table 26.11-1*)

$\bar{z}$: Equivalent height of the building is defined as $0.6h$

β: Damping ratio, 1.5% typical for steel-framed buildings.

ε: $1/5.0$ (*Table 26.11-1*)

l: 500 ft (*Table 26.11-1*)

$\bar{b}$: 0.66 (*Table 26.11-1*)

$\bar{\alpha}$: $1/6.4$ (*Table 26.11-1*)

From the listed equations, the final gust effect factor that will be applied to this building will be $G_f = 1.08$. The enclosure classification for this building can be justified as an enclosed building in which the internal pressure coefficient (GC_{pi}) can be taken as ± 0.18 from *Table 26.13-1*. With both factors being accounted for, Chapter 27 will be used to determine the wind pressures on the MWFRS in both windward, leeward, and sidewalls. The design wind pressure for the MWFRS for the high-rise structure will be defined by the equation:

$$p = qK_dG_fC_p - q_iK_d\left(GC_{pi}\right) \tag{20}$$

Where

$q = q_z$: For windward walls evaluated at height *z* above the ground

$q = q_h$: For leeward walls, sidewalls, and roofs evaluated at height *h*

$q_i = q_z$: For windward, sidewalls, leeward walls, and roofs of enclosed buildings

K_d: Wind directionality factor

G_f: Gust-effect factor

C_p: External pressure coefficient

(GC_{pi}): Internal pressure coefficient

A few factors will need to be determined to calculate the wind pressure per specified elevations. Going back to Chapter 26, *Table 26.6-1,* since the high-rise is classified as a main wind force resisting system, the wind directionality factor will be taken as 0.85. The external pressure coefficients will vary depending on which side the wind is directed; *Figure 27.3-1* can be used to determine the coefficients. For windward and sidewall, the coefficient will be 0.8 and -0.7, respectively. As for the leeward wall, it is dependent on the ratio of the length compared to the base. The high-rise case study structure will have a base-to-width ratio of 1.0, meaning that the leeward coefficient will be -0.5 per ASCE 7-22 *Figure 27.3-1*. With all unknown values being determined, the total wind pressure can be calculated for each interval of 20 ft. Figure 1 illustrates the total wind pressure experienced at each side of the structure.

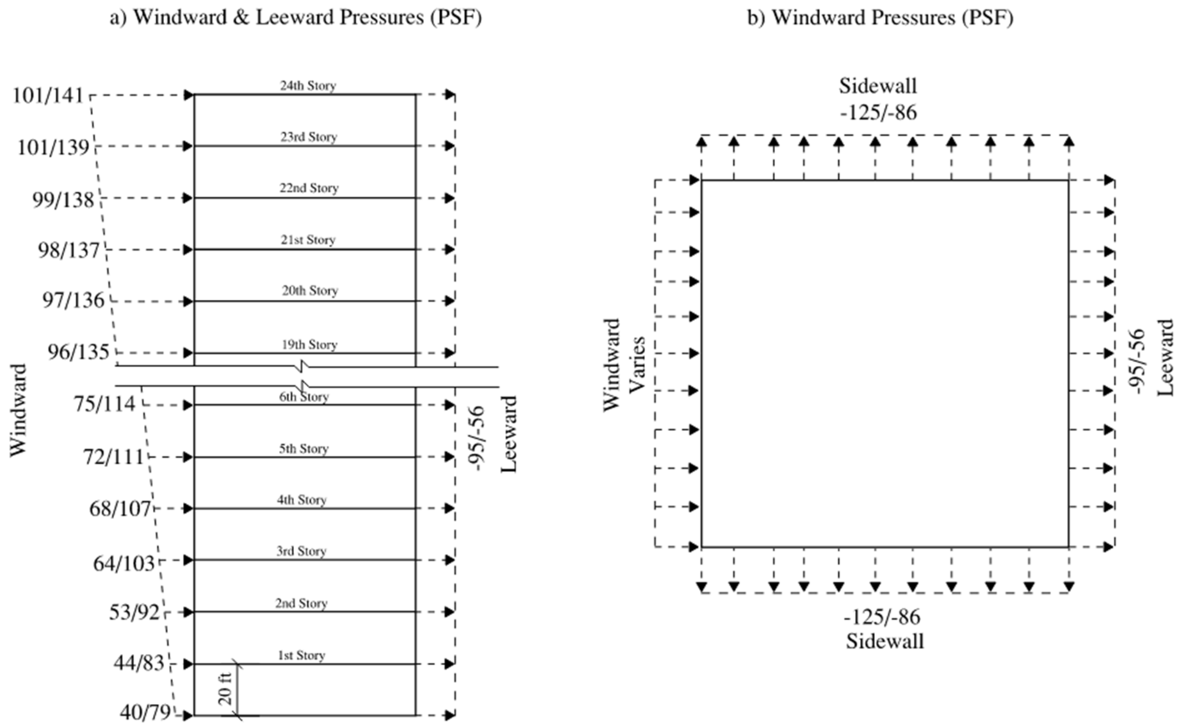

Figure 1: Wind Diagram for Structural Case

Two forces need to be considered for comparison to additional wind forces; the first being the sidewall forces. The negative values expressed in the diagram represent a suction force along the walls. This means the force the sidewalls experience will be a maximum of 7224 kips and a minimum of 4972 kips (derived by multiplying the side wall pressures by the area of the side walls) directed outwards from the center of the structure. This sidewall force value will serve as the baseline for evaluating the impact of additional wind effects from conditions such as vortex shedding. The second force will be the overall base shear calculated by taking the average windward pressure at each floor, adding the absolute value of the corresponding leeward pressure, and multiplying the result by the total tributary wall area at each elevation (2400 ft^2). Summing up the lateral forces across all levels, the total base shear for the structure was determined to be 10,168 kips. This can be used in comparison to methods that address the wind acting along the windward side, such as dynamic amplification. These values will serve as the baseline for evaluating the impact of additional wind effects not explicitly addressed in ASCE 7-22. The additional aerodynamic wind effects will be defined and applied to the same high-rise case study structure to assess whether they introduce significant additional forces that could alter the overall exterior wind force.

Chapter 3: Additional Wind Effects

3.1.0 Vortex Shedding Overview

Vortex shedding is a phenomenon in which alternating vortices are shed from the sides of high-rise buildings in a uniformly steady wind. Through these alternating vortices, a periodic force is created that can cause the building to sway or oscillate in addition to the preexisting wind pressure. To apply this idea to the predetermined high-rise case study structure, an understanding is needed that, as wind flows past a rectangular building, the boundary layer will begin to separate at the edges, producing an alternating vortex. This phenomenon is known as the Von Karman vortex street; this effect produces a suction pattern that fluctuates on the sides of the building, resulting in a lateral force acting perpendicular to the average wind direction (*Lopatinski, 2020*).

The forces that would be generated by vortex shedding differ from the predetermined force addressed in ASCE 7-22, specifically in Chapters 26 and 27. ASCE 7-22 provisions equations were used to determine wind loads that are static along the structure using the velocity pressure, exposure coefficient, and gust factors. However, ASCE 7-22 does not explicitly incorporate the vortex-induced oscillations acting perpendicular to the wind direction, which can become critical when the vortex shedding frequency reaches the fundamental natural frequency of the high-rise structure (*Lopatinski, 2020*).

Due to this interaction between vortex shedding and dynamics, it is necessary to evaluate the wind force attributable to vortex-induced forces. Determining this additional force provided the means of comparing it to ASCE 7-22 static wind loads to see if the ASCE 7-22 calculated values are considered conservative. The vortex force can be combined directly with the ASCE sidewall force since they will both be acting in the perpendicular wind direction.

3.1.1 Vortex Shedding Equations

To calculate the force attributed by vortex shedding, the use of equations outlined in both *Vortex Induced Vibrations in High-Rise Buildings (Lopatinski 2020)* as well as *Eurocode 1: Actions on Structures-Part 1-4: General Actions – Wind Actions (EN 1991-1-4)* will be used for calculation comparison purposes. The first calculation needed to be determined is the shedding frequency to compare to the building's natural frequency to see if the oscillation is critical. To do this, the standard equation for shedding frequency will be used:

$$f_s = \frac{St\,U}{d} \tag{21}$$

Where

St: Strouhal Number (Figure 2)

U: Velocity of wind

d: Across-wind dimension of the structure

Since the high-rise case study structure has a square cross-section and is assumed to have sharp corners, the Strouhal Number will be determined using Figure 2. This figure is taken from the EN 1991-1-4 *Eurocode 1: Actions on Structures – Part 1-4: General Actions – Wind actions.*

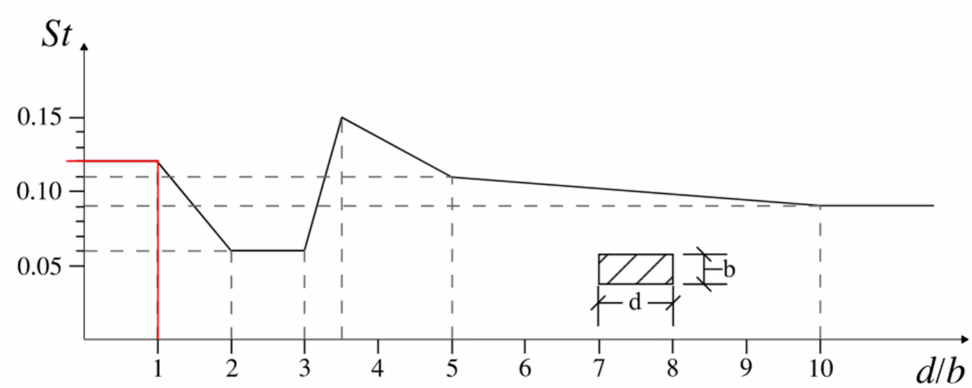

Figure 2: Strouhal number (St) for rectangular cross-sections with sharp corners (Adapted on EN 1991-1-4:2005)

With the d/b ratio being 1, the Strouhal number will be taken as 0.12. Through the use of Equation 21, the overall shedding frequency was 0.249 Hz, which is more than the structure's natural frequency set at 0.158 Hz from Equation 4, resulting in this building being considered in critical oscillation per *Lopatinski (2020)*. The fluctuating load per unit height (F) of the structure is determined by the following equation:

$$F = \frac{1}{2}\rho U^2 b C_{L,rms} h \qquad (22)$$

Where

ρ: Air density ($0.0765\ \mathrm{lb/ft^3}$)

U: Velocity of wind (170 mph)

b: Across-wind dimension of the structure (ft)

$C_{L,rms}$: Coefficient of lift, (1.10 per EN1991-1-4)

h: Building height (ft)

Using the full height of the case study structure, the total vortex shedding force was found to be overly conservative, due to the fact that it assumes the lift coefficient is constant throughout the full building height. This is largely unrealistic since, in most cases the structure would experience the lift at sections not along the full face of the windward side. In order to adjust this factor, the vortex shedding force will need to be changed to a more reasonable consideration using the methods *Lopatinski (2020)* discusses. These methods adjusted the fluctuating load per unit height (F) by applying the modal project factor, coherence, forcing peak, and dynamic amplification.

Currently, the entire vortex load is assumed to act in perfect phase with the building's first mode; realistically, only a fraction of the distributed across-wind force projects onto the first mode of the structure. Because of this, a modal project factor can be applied to the building to help reduce the force. By treating the building as a vertical cantilever beam under vibration and simplifying the equations derived by *Lopatinski (2020),* as well as standard cantilever function expressions, the modal projection factor (p) of the normalized mode shape is as follows:

$$p = \int_0^1 \phi_n(\xi)\, d\varepsilon \tag{23}$$

The normalized mode shape expression [$\phi_n(\xi)$] of the structure will be represented by the closed-form expression for the mode shape of the n-th bending mode of a uniform vertical cantilever. Where α is the non-dimensional eigenvalue and β will represent the shape coefficient of the slope at the free end, in which boundary conditions are satisfied.

$$\phi_n(\xi) = \frac{\phi(\xi)}{\phi(1)} \tag{24}$$

$$\phi(\xi) = \cosh(\alpha\xi) - \cos(\alpha\xi) - \beta(\sinh(\alpha\xi) - \sin(\alpha\xi)) \tag{25}$$

$$\cos(\alpha)\cosh(\alpha) + 1 = 0 \tag{26}$$

$$\beta = \frac{\cosh\alpha + \cos\alpha}{\sinh\alpha + \sin\alpha} \tag{27}$$

$$\xi = \frac{z}{h} \tag{28}$$

Where

z: Height above ground level

h: Total building height

The normalized mode shape was evaluated over the total building height, corresponding to $\xi = 0$ at ground level and $\xi = 1$ at the roof. Using numerical integration to apply 1,000 iterations to get as precise as possible, the modal project factor was determined to be around 39% of the uniformly distributed force acting on the first mode's dynamic response. By applying this to the vortex shedding force, it reduces the overall force to a more reasonable adjustment. This is a sufficient starting force, but another way to reduce this will be to consider the coherence of the building. Coherence states that when the wind is flowing past the building, vortices are shed along the height. These vortices are not in perfect sync at each elevation, meaning the motion (or vibration) is partially correlated from one level to the other. The current vortex force assumes that the shedding is vibrating equally along the full building height when, realistically, only a portion will be in sync. To determine a more accurate assumption, the coherence will be taken from a range of 10-30%. This will result in the force now being reduced to the coherence percentage (a full breakdown table presented within Chapter 4.2 of the report). This new force is a more realistic value when compared to the initial value calculated from Equation 22. Before it can be added to ASCE 7-22 wind pressure, however, two additional considerations need to be made to better represent the maximum vortex shedding force, also known as the worst-case force. The first will be to apply what is considered the peak-factor (k_p), the general expression of peak-factor is:

$$k_p = \sqrt{2\ln(\tau T)} + \frac{0.5772}{\sqrt{2\ln(\tau T)}} \tag{29}$$

Where

τ: average up-crossing frequency (same as f_s)

T: sample time (10 minutes will be used)

Using the shedding frequency and a time of 10 minutes, the peak factor will be 3.35, which results in a vortex force increasing to account for the worst case in which the wind is at constant max speed or peak force. The last factor that needs to be considered will be the vortex shedding's dynamic amplification on the structure. If the shedding frequency is close to the structure's natural frequency, then the structure will resonate. Since the high-rise case study structure's natural frequency (0.158 Hz) is smaller than the shedding frequency (0.249 Hz), the structure is considered in critical oscillation, and the dynamic amplification will represent the vibrational amplitude associated. To determine the amplification factor, the equation of a single degree of freedom will be used:

$$r = \frac{f_s}{f_n} \tag{30}$$

$$DAF = \frac{1}{\sqrt{(1-r^2)^2 + (2\zeta r)^2}} \tag{31}$$

Where

f_s: shedding frequency

f_n: building's natural frequency

ζ: damping ratio (assumed 1.5% for this building)

The amplification factor for this high-rise case study structure was calculated to be 0.68. With additional factors being considered in the structure, the vortex force can be compared to the ASCE 7-22 sidewall pressure. The shedding loops the wind force to act in compression along the sidewalls, which counteracts the suction force calculated from ASCE 7-22. Since both forces, ASCE 7-22 sidewall and vortex shedding force, are acting in the same direction, they can be directly compared, with ASCE 7-22 being in tension and vortex shedding being in compression. The maximum ASCE 7-22 tension force of 7224 kips will be used in the calculation to determine the worst-case scenario. By taking the ratio of the ASCE 7-22 sidewall force and the vortex shedding force the additional sidewall force percentage can be determined.

$$V_{add'l} = \frac{V_{Vortex}}{V_{ASCE}}(100) \tag{32}$$

3.1.2 Vortex Shedding Summary

Looking at the mathematical approach of applying vortex shedding to high-rise structures, the total resultant force at 10% coherence will be considered a reasonable and conservative representation of the effects of vortex shedding on the ASCE 7-22 wind force calculations. With this, it should be noted that the sidewall pressure experienced an additional compressive force of by 5.8% compared to the base ASCE 7-22 sidewall force. While vortex shedding is not a governing consideration in most structural design applications, when looking at buildings classified as high-rise structures, additional considerations could be made to best optimize designs.

3.2.0 Dynamic Amplification

An additional modification that may result in a change in the base shear would be the dynamic amplification due to translational response. When the wind loading is acting at or near the natural frequency of the building, dynamic amplification can occur, which can lead to an increase in the structural response. Unlike static wind loading, dynamic amplification doesn't assume a uniform pressure distribution; instead, it looks at the fluctuating wind pressures and how the building will resonate.

For translational dynamic amplification, the ASCE 7-22 version accounts for part of this behavior through the use of the gust effect factor for both rigid and, in this case, flexible buildings. However, the gust effect factor assumes a simplified single degree of freedom translational response and doesn't use explicit dynamic analysis for any resonant effects. In their respective research, "*Wind Loads and Dynamic Responses of Tall Buildings"*, *Boggs and Dragovich (2006)* and *"Dynamic Response of Tall Buildings to Wind Excitation" Torkamani and Pramono (1985)*, both demonstrated that for tall buildings, the resonant component of wind may increase the overall base shear compared to methods similar to the ASCE 7-22 procedure.

The following section will break down the approach to solve for a base shear using the understanding and formulated equations from different research within the field of gust effects and dynamic response due to wind. This base shear from dynamic amplification will be compared to that calculated from Chapter 2 using the ASCE 7-22 method and equations.

3.2.1 Translational Amplification Equations

Before breaking down modifications to the base shear, an understanding needs to be made regarding gust effect factors. Currently, the ASCE 7-22 gust effect factor that was applied to the high-rise case structure takes into account wind speed and the maximum expected wind response to the mean wind response. Although the traditional gust effect factor method ensures an accurate estimation of the displacement response, it may fail to properly represent other response components. To counter this, a procedure for determining design loads on tall structures was proposed by *Kareem & Zhou (2003)*, in which the gust loading factor is based on the bending moment at the base rather than the displacement. This factor for simplicity will be noted as the response gust factor and be represented with the variable; G_M. To refine what the response gust factor could look like using the topic of dynamic amplification the first step will be to take the predetermined equation of motion for a single degree of freedom system and modify it to work more efficiently within the case structure. A diagram produced by *Kareem & Zhou (2001)* breaks down the probabilistic-based approaches to gust loading factors through the use of a displacement or moment factor model.

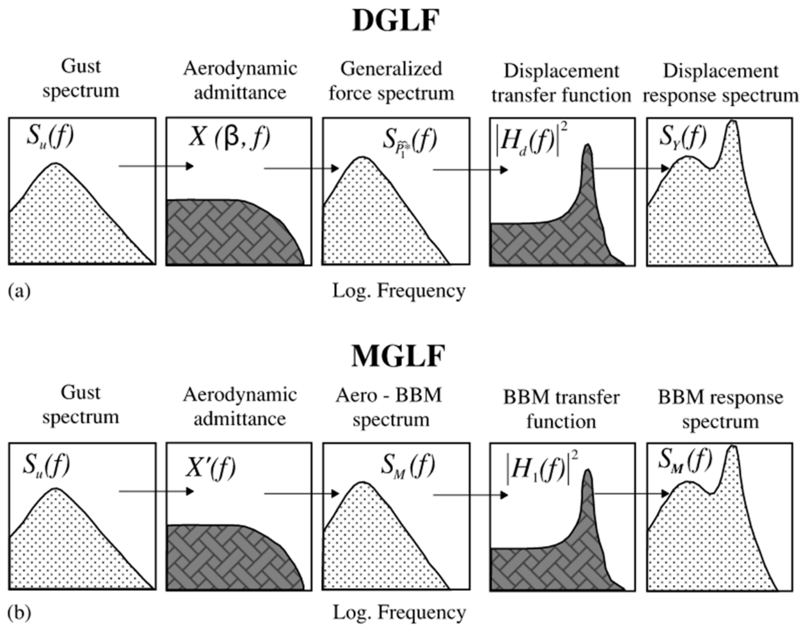

Figure 3: Probabilistic-Dynamic Based Approaches to Gust Loading (Adapted from Kareem & Zhou (2001))

Using the understanding from research done by *Boggs and Dragovich (2006)* to convey the dynamic response to wind loading in mathematical terms, if the excitation of the single degree of freedom (SDOF) system is sinusoidal (force that varies in a regular wave-like pattern) the equation of motion will be:

$$m\ddot{x} + c\dot{x} + kx = P_0 \sin 2\pi ft \qquad (33)$$

Where

m: generalized mass

c: viscous damping coefficient

k: stiffness coefficient

P_0: initial loading

ft: frequency

When a steady state solution $[x(t) = x_0 \sin(2\pi f t - \psi)]$ is applied to the aforementioned equation of motion, it allows the complex systems to be simplified to the magnitude of the internal response force, which can be expressed as:

$$\boldsymbol{P} = |H(f)|P \tag{34}$$

Where

$$|H(f)|^2 = \frac{1}{\left(1 - \left(\frac{f}{f_0}\right)^2\right)^2 + \left(2\xi \frac{f}{f_0}\right)^2} \tag{35}$$

This expression of $|H(f)|$ is regarded as the mechanical admittance which can be used to determine how easily a system's motion can respond to an applied force. If the exciting frequency (f) is close to the natural frequency (f_0) and the damping (ξ) is low, the function is known as resonance, similar to the dynamic amplification factor talked about within the case of vortex shedding. This always occurs to some extent in a flexible building under wind loading. Since wind excitation is not sinusoidal but instead consists of a broad range of different frequencies undergoing random superposition. Due to this, a power spectral density equation for the response can be created which describes how the response of a signal is distributed over a frequency.

$$S_{\boldsymbol{P}^*}(f) = |H(f)|^2 S_P(f) \tag{36}$$

Where

S_{P^*}: generalized response load

S_P: simple response load

In the paper by *Boggs and Dragovich (2006),* they state that the response should be considered the superposition of two components, namely background and resonance. The background refers to the static response to the fluctuating portion of the frequency of the wind load, if the frequency of the wind load is high. The resonance represents the additional amplification that is embedded in the $|H(f)|$ function and may be considered the dynamic response to the wind gusts having a duration close to the natural period of the structure. The fluctuating response can be obtained using integration of the power spectral density equation.

$$\sigma_{P^*}^2 = \int_0^{\infty} |H(f)|^2 S_P(f)\, df \tag{37}$$

Boggs and Dragovich (2006) stated in their research "Under particular yet common conditions this can be represented by the well-known white noise approximation, avoiding the integration indicated in the power spectral density equation" (Equation 37).

$$\sigma_{P^*,R} = \sqrt{\frac{\pi}{4\xi} f_0 S_P(f_0)} \tag{38}$$

In order to determine the new gust loading factor as a basis of bending moment rather than displacement, a proposed approach by *Kareem & Zhou (2003)* in their research, "*Gust Loading Factor: New Mode*", was created to form the equation:

$$G_M = 1 + \frac{g_M \sigma_{\bar{M}}}{\bar{M}} \qquad 39(a)$$

Where

g_M: peak factor

$\sigma_{\bar{M}}$: Root mean square base bending moment

The base bending moment includes the effects of turbulence structure interaction, and the development of the root mean square base bending response is similar to the development of the white noise approximation mean. To simplify the gust loading factor, the substitution of the two responses as well as mathematical manipulations simplifies Equation 39 (a) to be:

$$G_M = 1 + 2I_H\sqrt{g_u^2 B + g_R^2 R} \qquad 39\ (b)$$

Where

I_H: turbulent intensity evaluated at the top of the structure

g_u: wind velocity peak factor (typically 3.4)

g_R: resonance peak factor (taken at 10 minutes)

B: background response factor

R: resonance response factor

The breakdown of the unknown variables in the moment gust loading factor (MGLF) will be as follows:

$$I_H = \frac{\sigma_u}{\overline{U}_H} = \frac{1}{\ln(H/z_0)} \qquad (40)$$

$$g_R = \sqrt{2\ln(f_1 T)} + \frac{0.5772}{\sqrt{2\ln(f_1 T)}} \qquad (41)$$

$$B = \int_0^\infty \left[\frac{2(1+\alpha)}{2+\alpha}\right]^2 \left|\exp\left(-11.5\frac{fH}{\overline{U}_H}\right)\right|^2 \left|\frac{2}{(2+\alpha)}\frac{1}{1+\left(\frac{11.5fH}{\overline{U}_H}\right)^2}\right|^2 \left[\frac{16H}{0.12\overline{U}_H\left(1+\frac{16H^2}{0.0144\overline{U}_H^2}\right)^{\frac{4}{3}}}\right] df \qquad (42)$$

$$R = \frac{S(\pi f_1)}{4\zeta} \qquad (43)$$

Where

H: building height

z_0: standard roughness length (Exposure C = 0.098 ft)

f_1: natural frequency (0.158 Hz)

T: observation time (10 minutes)

$\overline{U}_H$: mean wind velocity (170 mph)

α: standard exponent (Exposure C = 0.16)

S: size reduction factor

ζ: damping ratio (1.5%)

The use of Equations 42 and 43 could be used to determine the background and resonance factor, but within their paper, *Kareem & Zhou (2003)* state: “For code application of the MGLF, *B* and *R* can be obtained from graphs or closed-form expressions like the ones used in the DGLF”. Since all factors have been calculated in Chapter 2, for simplicity and to help reduce the potential error *B* = 0.806 and *R* = 1.79 (from Chapter 2, Section 1 of this report) will be used for the background and resonance factors respectively. From which the moment gust loading factor was calculated using the aforementioned values and the resonance peak factor. The next step, as described by *Kareem & Zhou (2003),* will be to determine the extreme moment by multiplying the mean base moment by the MGLF. The base moment can be computed by taking the integral of the mean wind load equation:

$$\bar{M} = \int_0^H \frac{1}{2}\rho C_D W \bar{U}_H^2 \left(\frac{z}{H}\right)^{2\alpha} z\,dz = \frac{\frac{1}{2}\rho C_D W U_H^2 H^2}{2+2\alpha} \tag{44}$$

Where

C_D: drag coefficient (assumed 1.2)

ρ: air density ($0.076\frac{lbm}{ft^3}$)

W: width of the structure normal to the oncoming wind

Through the use of Equation 44, the base bending moment was determined to be 1,049,168 k-ft. To determine the extreme moment that will be used to determine the base shear, the bending moment ($\bar{M}$) was multiplied by the moment gust loading factor (G_M) which resulted in an adjusted moment of over 2,600,000 k-ft. To apply this new moment to a base shear equation, the assumption is that the wind load will be acting uniformly across the entire structure. Assuming a linear equivalent static wind load distribution consistent with the first mode shape, as implied by the moment gust loading factor (MGLF) formulation of *Kareem & Zhou (2001)*, the calculation for shear will be simplified to the equation:

$$V = \frac{2M_e}{H} \tag{45}$$

Where

M_e: extreme base moment

H: building height

3.2.2 Dynamic Amplification Summary

With the dynamic amplification method through the use of the moment gust effect factor the base shear was calculated to be 9848 kips. Dynamic amplification yielded around a 3.1% decrease in the overall base shear. Since the dynamic amplification base shear was determined through the use of calculations alone, the statement needs to be made that this value should be checked with the use of wind tunnel testing to potentially reduce some values, such as background and resonance response factors, and the peak factor would change if a different observation time were selected. Another factor when considering the validity of the results is the assumption that had to be made to simplify the base shear calculation. Wind loading is typically non-uniform when at high speeds and dependent of building shapes. In order to determine the shear based on limited information, a simplified equation was used but the true shear equation could be more complicated and yield a more accurate base shear percentage difference.

Chapter 4: Wind Effect Calculations

Chapter 4 will apply the numerical applications to the wind load methodologies introduced in the preceding chapters. A step-by-step calculation process is provided for both the ASCE 7-22 method equations and each additional wind effect not fully addressed in code allowing for a direct numerical comparison otherwise represented by a percentage change in the previous chapter.

4.1 ASCE 7-22 Calculations

The use of equations in Chapter 2 will be used to determine the representative value for the base shear that case study structure will experience. The structure was determined to be classified as a flexible structure using Equation 4.

$$n_1 = \frac{22.2}{480^{0.8}} = 0.158 < 1$$

With the flexible classification equations, 5-19 are needed to determine the gust factor effect. To simplify the overall numeric solutions, only a few equations will be mathematically shown through their respective equations, that being the gust effect factor G_f (eq 5), resonant peak factor g_R (eq 6), background response factor Q (eq 7), and resonant response factor R (eq 9). The remaining equations not listed were utilized but not shown numerically; their values will be used to solve the needed equations and are as follows: $I_{\bar{z}} = 0.139$, $R_n = 0.176$, $N_1 = 0.531$, $L_{\bar{z}} = 771.16$, $\bar{V}_{\bar{z}} = 230.83$, $R_h = 0.452$, $R_B = 0.788$, $R_L = 0.501$, $\eta_h = 1.52$, $\eta_B = 0.38$, and $\eta_L = 1.27$. With those values being listed, the 4 main equations are:

$$g_R = \sqrt{2\ln(3600(0.158))} + \frac{0.577}{\sqrt{2\ln\big(3600(0.158)\big)}} = 3.73$$

$$R = \sqrt{\frac{1}{0.015}(0.176)(0.452)(0.788)\big(0.53 + 0.47(0.501)\big)} = 1.791$$

$$Q = \sqrt{\frac{1}{1 + 0.63\left(\frac{120 + 480}{771.16}\right)^{0.63}}} = 0.806$$

$$G_f = 0.925\left(\frac{1 + 1.7(0.139)\sqrt{3.4^2(0.806)^2 + 3.73^2(1.791)^2}}{1 + 1.7(3.4)(0.139)}\right) = 1.39$$

With the gust factor effect determined, the wind pressure can be calculated for each elevation using two equations, Equation 1 calculating the velocity pressure and Equation 20 to determine the wind pressure for windward/leeward/and sidewalls. The calculations will be the same process with the only variable changing being the elevation change on intervals of 20ft. *Table 1: Velocity Pressure Per Elevation* expresses each pressure at its respective elevations. A sample calculation at 100 ft will be shown to understand the numeric breakdown for the wind pressure.

$$q_z = 0.00256(1.254)(1.0)(1.0)(170)^2 = 92.75\, psf$$

$$p = 92.75(0.85)(1.39)(0.8) - 127.74(0.85)(\pm 0.18) = 101.5/140.5\, psf$$

Figure 1: Wind Diagram for Structural Case shows the windward pressure for each elevation utilizing the equations above. With all the wind pressures determined, the remaining equations needed to be used for the ASCE 7-22 section will be the equation to determine the base shear for the overall structural case, as well as the side wall force experienced. While the base

shear equation isn't listed it is a fundamental equation which sums the averages of each windward pressure (in psf) at the level above and below added to the leeward pressure and multiplied by the surface area of the windward face, starting at the 24th story all the way to the 1st with the windward pressure at the 1st story windward pressure being directly added to the leeward pressure. The overall expression for the base shear is represented as follows:

$$V_{base} = \left[\left(\frac{101.5 + 100.4}{2} + 95.2\right) + \left(\frac{100.4 + 99.3}{2} + 95.2\right) + \cdots + (43.7 + 95.2)\right](2400ft^2)$$

$$\boldsymbol{V_{base} = 10168\ kips}$$

As for the sidewall force, it is a simpler solution, only requiring the ASCE 7-22 sidewall force maximum of -125.42 psf to be multiplied by the sidewall area of 57600 square feet.

$$V_{sidewall} = -125.42\,psf(57600\ ft^2) = \boldsymbol{7224\ kips\ (Tension)}$$

The high-rise case study structure is experiencing a base shear of around 10168 kips when using the current ASCE, which will be the reference force for comparison to the additional wind effect caused by dynamic amplification. While the sidewall will experience a force of 7224 kips of tension, which will be compared to the vortex shedding forces.

4.2 Vortex Shedding Calculations

Chapter 3 describes the necessary equations to determine the additional sidewall force created by the introduction of vortex shedding. The first critical calculation is Equation 21, since it will determine if the structure experiences critical oscillation. It was stated that the shedding frequency was more than the natural frequency ($f_1 = n_1 = 0.158\ Hz$). The exact shedding frequency was based on the Strouhal Number (0.12) determined from *Figure 2 -Strouhal number*

(St) for rectangular cross-sections with sharp corners (EN 1991-1-4:2005) and the ratio of the length to base of the structure being 1.0, resulting in:

$$f_s = \frac{0.12\left(249.33\,\frac{ft}{sec}\right)}{120\ ft} = 0.249\ Hz$$

The force on the building by vortex shedding will be calculated using Equation 22. The whole building height is 480 ft, and a lift coefficient of 1.10 is taken from the *Eurocode 1: Actions on Structures – Part 1-4: General Actions – Wind actions*. This value is standard for most square structures, which is what the case study structure is classified as; the force on the building will be:

$$F = \frac{1}{2}\left(0.0765\,\frac{lbm}{ft^3}\right)\left(249.33\,\frac{ft}{sec}\right)^2(120ft)(1.10)(480ft)\left(\frac{1\ lb}{32.2\,\frac{lbm\ ft}{sec^2}}\right) = 4679\ kips$$

As stated in Chapter 3, this value is considered unrealistic and will need to be reduced using factors such as modal project factor, coherence, forcing peak, and dynamic amplification. These concepts were discussed within *Vortex Induced Vibrations in High-Rise Buildings (Lopatinski 2020)* and explained further in Chapter 3. The first reduction factor that will be applied is the modal project factor through the use of eq 23-28. Since the most precise factor is needed, the modal projection integral was computed through 1,000 iterations using an integral calculator with lengths increased by 0.001. The following table (Table 2) will represent a portion of the integration steps to show the process to determine the overall modal projection factor using $\alpha = 1.875$ and $\beta = 0.734$.

Table 2: Modal Projection Factor Integration

x_{start}	x_{end}	$\phi_{n,start}$	$\phi_{n,end}$	Area Segment	Cumulative Area %
0	0.001	0	1.7572E-06	8.7860E-10	8.7860E-10
0.001	0.002	1.7572E-06	7.0256E-06	4.3913E-09	5.2699E-09
0.002	0.003	7.0256E-06	1.5800E-05	1.1413E-08	1.6683E-08
0.003	0.004	1.5800E-05	2.8077E-05	2.1938E-08	3.8621E-08
0.004	0.005	2.8077E-05	4.3849E-05	3.5963E-08	7.4584E-08
…….					
0.996	0.997	0.994494	0.995870	0.000995	0.3885
0.997	0.998	0.995870	0.997247	0.000996	0.3894
0.998	0.999	0.997247	0.998623	0.000997	0.3905
0.999	1.00	0.998623	1.00	0.000999	0.3915

Through integration, the modal projection factor reduced the shedding force to 39.15% of the original value. That means the 4679 kips of force computed by the vortex shedding will be reduced to 1832 kips acting along the structure, which will be modified further through additional factors. The first being the coherence, as stated in chapter 3, the coherence that will be applied to this structure will be between 10-30% to show the level difference. This range means the 1832 kips from the modal projection factor will be reduced to a range of 183-549 kips. To make the range of values represent the maximum force the structure experiences, the peak factor needs to be computed and applied using Equation 29, with a sample time of 10 minutes and the shedding frequency calculated earlier at 0.249 Hz.

$$k_p = \sqrt{2\ln\big(0.249\ Hz\ (600\ sec)\big)} + \frac{0.5772}{\sqrt{2\ln(0.249\ Hz\ (600\ sec))}} = 3.35$$

This peak factor increases the force range to 613-1839 kips. The last factor needing to be applied is the vortex shedding's single-mode dynamic amplification mentioned in Chapter 3. The ratio of 1.57 between the shedding frequency, the structure's natural frequency, and the damping ratio is considered a very small resonance occurring throughout the structure. The use of Equations 30 & 31 will be used to determine the amplification factor that will be applied to the shedding force range, while small changes will still affect the overall force.

$$r = \frac{0.249}{0.158} = 1.57$$

$$DAF = \frac{1}{\sqrt{(1 - 1.57^2)^2 + (2(0.015)(1.57))^2}} = 0.685$$

This amplification factor increases the range of force values to be 420-1259 kips. With all factors applied to the original shedding force, the increase in base shear can be determined using the method described in Chapter 3 using Equation 32. *Table 3* will show the resultant force (total sidewall shear) for each coherence level from 10-30%. Note that only 10% will be mathematically shown, and all coherence percentages result in forces that will be in tension.

$$V_{add'l} = \frac{419.89\ kips}{7224.04\ kips}(100) = 5.81\%\ additonal\ force$$

Table 3: Resultant Forces Due to Additional Vortex Effects

Coherence (c)	Vortex Force (kips)	Modal Project Factor (p=0.39) (kips)	Peak Factor (k_p=3.35) (kips)	Amplification Factor (DAF=0.68) (kips)	Additional Force $V_{Add'l}$ (%)
10%	468	183	613	420	**5.8**
15%	702	275	920	630	**8.7**
20%	936	366	1226	840	**11.6**
25%	1170	456	1533	1050	**14.5**
30%	1404	550	1839	1260	**17.4**

Looking at the additional forces, they will all be in tension, but there is a noticeable addition in the sidewall force. For the use of this report, only the additional force calculated at 10% coherence (420 kips, 5.8%) will be used for the final comparison due to the uncertainty within the mathematical approach. A more refined value should be computed through the use of wind tunnel testing, but this report will only focus on hand calculations.

4.3 Dynamic Amplification Calculations

Using the equations broken down within the dynamic amplification section of Chapter 3, the main calculation needed will be the gust loading factor using Equation 39b. As established within that section, the background and resonance response factors will be taken from the ASCE 7-22 calculation to avoid errors; 0.806 and 1.791 will be used, respectively. The resonant peak factor and turbulent intensity will be computed using Equations 40 and 41, with the peak factor based on a 10-minute interval:

$$I_H = \frac{1}{\ln\left(\frac{480ft}{0.098ft}\right)} = 0.118$$

$$g_R = \sqrt{2\ln(0.158(600))} + \frac{0.5772}{\sqrt{2\ln(0.158(600))}} = 3.21$$

$$g_u = 3.4$$

This allows for the gust loading factor to be calculated using Equation 39b. This value will be utilized to determine the total base bending moment.

$$G_M = 1 + 2(0.118)\sqrt{3.4^2(0.806) + 3.21^2(1.791)} = 2.25$$

To apply the gust loading factor to the base bending moment, the standard moment caused by the wind will be determined through Equation 44:

$$\bar{M} = \frac{0.076\frac{lbm}{ft^3}(1.2)(120\ ft)\left(249.33\frac{ft}{s}\right)^2(480\ ft)^2\left(\frac{1\ lbf}{32.2\frac{lbm\ ft}{s^2}}\right)}{2(2+2(0.16))} = 1{,}049{,}169\ k-ft$$

Note that with both the moment and gust loading factor, the total base moment will be the product of the two, resulting in:

$$M = 2.25(1049168.86\ k-ft) = 2{,}363{,}726\ k-ft$$

With the base bending moment calculated, the last step will be to convert it into a form of base shear to compare to ASCE. By assuming a linear equivalent static wind load distribution, the conversion of base bending moment to base shear was formulated in Equation 45.

$$V = \frac{2(2363726\ k - ft)}{(480\ ft)} = \boldsymbol{9849\ kips}$$

Chapter 5: Potential Design Guide and Conclusion

With the additional wind effects accounted for, the comparison can be made between the code-based approach of ASCE 7-22 and the vortex shedding and dynamic amplification (MGLF). Looking at the vortex shedding, the 10% coherence will be considered a reasonable and conservative representation of the effect, resulting in a compression force of 420 kips. The new force will be in additional to the already existing ASCE 7-22 sidewall force of 7224 kips acting in tension. Since the ASCE 7-22 sidewall force acts on both sides, it will be assumed that ASCE 7-22 forces cancel with itself resulting in the vortex shedding being the additional force not counteracted. It should be noted that the sidewall compression pressure increased by 5.8% when vortex shedding was considered; this compression increase is quite noticeable when looking at the total force loading along the sidewalls. The increase in compression forces suggests that traditional code-based wind loading procedures may be conservative in cases where vortex shedding alters the force distribution. While such optimization is beyond the scope of this report, by accounting for this reduction in the sidewall force suggests that the overall framing system, such as moment frames or braced frames, used to resist sidewall moments could be optimized, and possible reduced member sizing could be implemented to save construction costs and member self-weight.

When looking at dynamic amplification, specifically MGLF approach, the new base shear calculated was 9849 kips. When compared to the displacement gust loading factor (DGLF) base shear from ASCE 7-22, there was a decrease of 3.14%. What this means is the code-based approach may overestimate the force loading however, note that the effect of MGLF on force-based responses is not unidirectional and depends on the relative contributions of background and resonant components as well as the structural characteristics. Although, the high-rise case structure used experiences a decrease in the base shear the MGLF could potentially increase the shear as well. This complicates the understanding as it could mean the DGLF or code-based approach may both underestimate or overestimate the shear depending on how its applied to the project.

To help break down and apply the mathematics discussed in this report to other design structures, a flow chart was created for vortex shedding. The goal is to simplify the approach and make it easier to apply to other high-rise designs. With the use of the flow chart, small checks can be made to understand what additional wind effects may be applicable to a design structure, making it easier to apply to other high-rise structures. With the use of the flow chart, small checks can be made to understand what additional wind effects may apply to a design. Figures 4 and 5 were created to show the step breakdown of each additional effect.

Vortex Shedding Design Flowchart

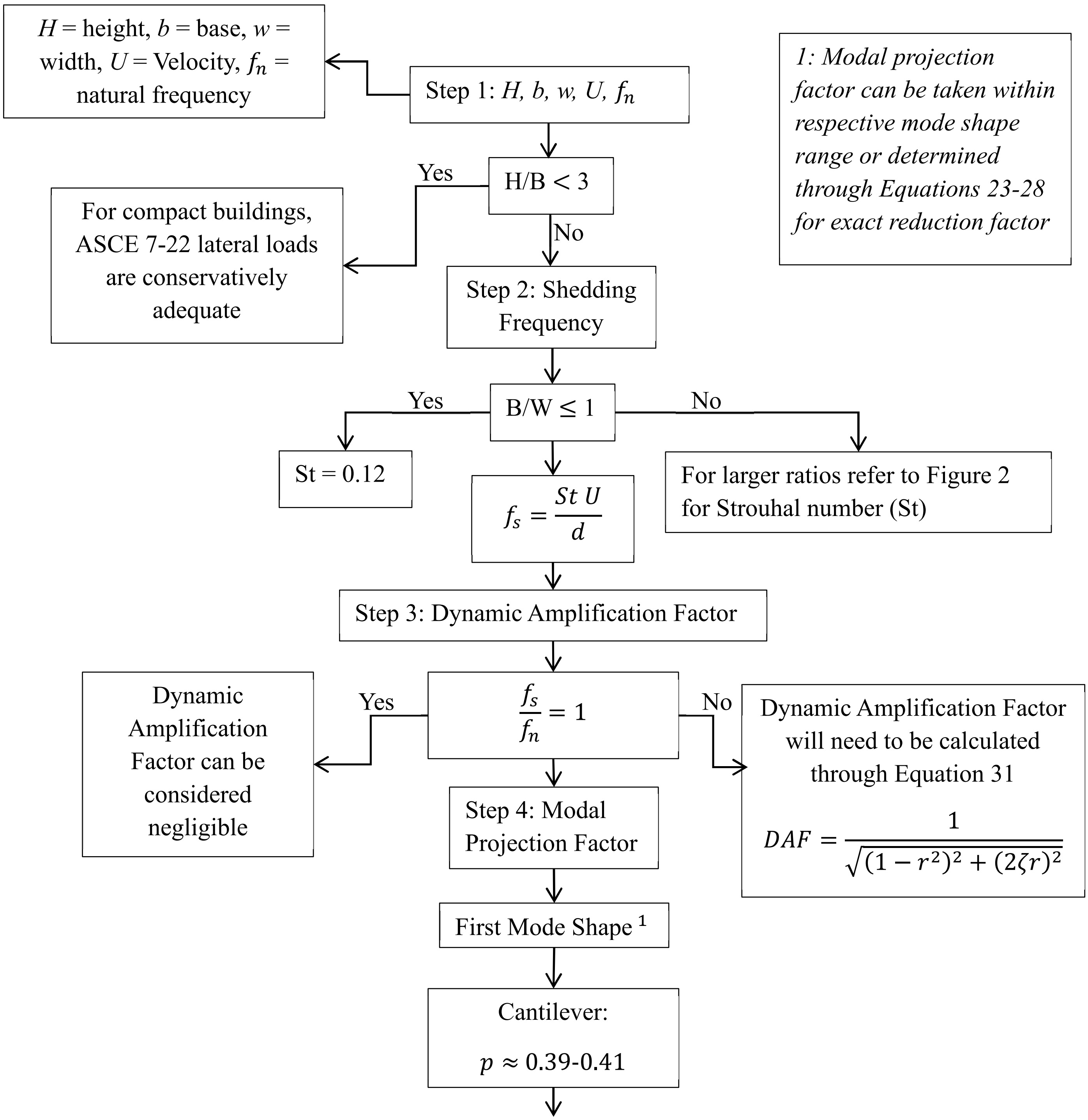

Vortex Shedding Design Flowchart (cont.)

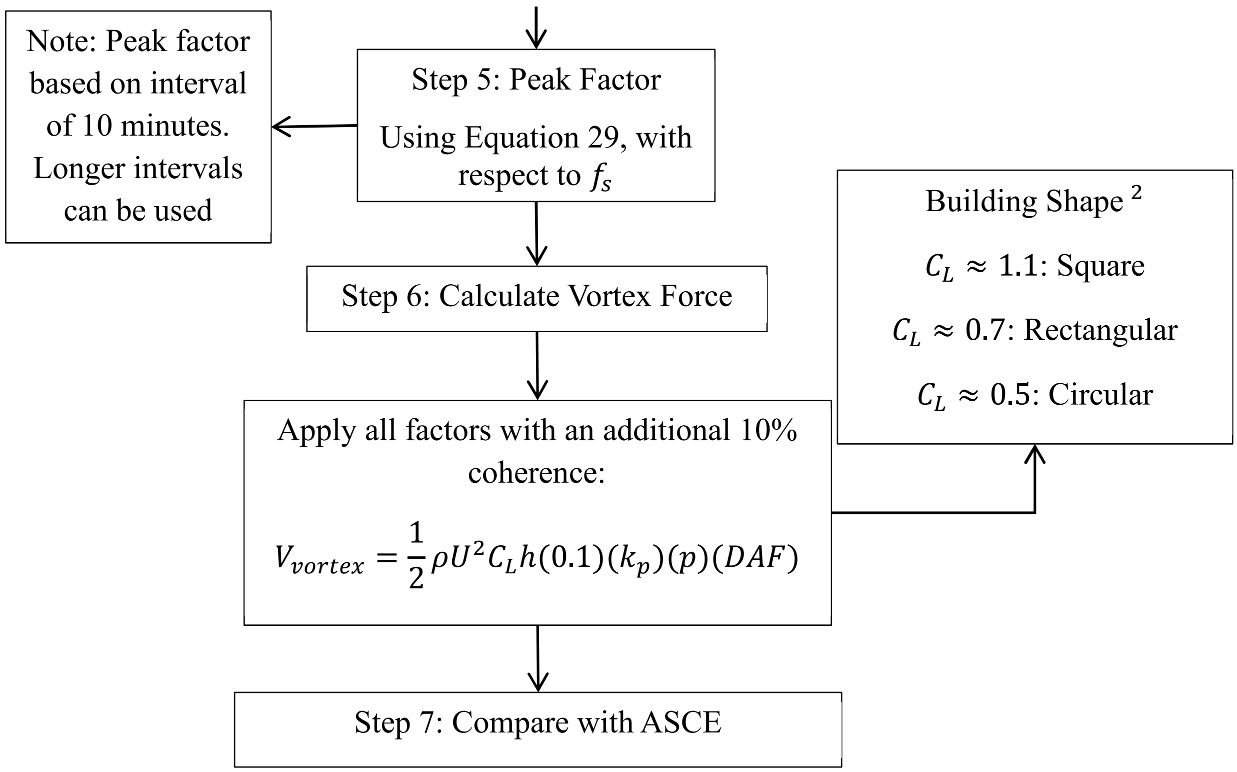

2: These lift coefficients values are approximate screening consistent with general vortex shedding trends. Eurocode EN 1991-1-4 addresses vortex shedding through dynamic response models with shape-dependent aerodynamic constants rather than static lift coefficient tables. Refer to Annex E for shape constants used in dynamic vortex response calculation.

Figure 4: Vortex Shedding Flowchart Design Guide

A similar approach was made for dynamic application, with Figure 5 being created to help apply the change in base shear from the moment gust loading factor addressed in Chapter 3, Section 2.0.

Dynamic Amplification Design Flowchart

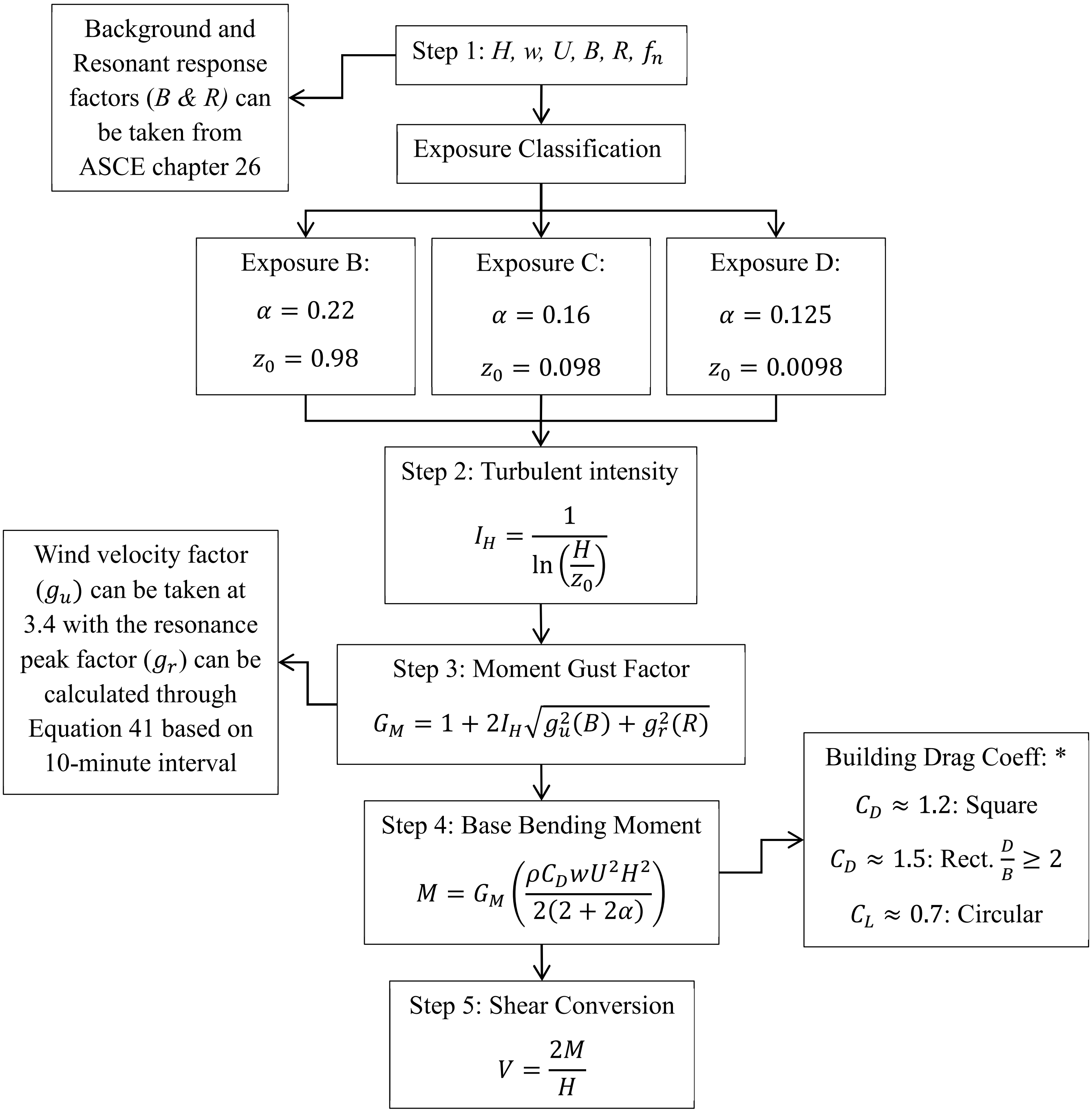

**: Drag coefficients are treated as effective engineering estimates; refinement would require geometry-specific aerodynamic evaluation such as wind tunnel testing.*

Figure 5: Dynamic Amplification Flowchart Design Guide

5.1 Design Guide Application

With the design guides created for the vortex shedding and dynamic amplification, it can be used for future high-rise structural designs. To show this, an additional high-rise structure will be looked at to see the forces created by vortex shedding and dynamic amplification. This high-rise will have dimensions of 120 ft x 240 ft x 640 ft tall. The exposure classification will be B with the wind velocity set at 145 mph; the frame will be set as a concrete moment resisting frame with the damping ratio of 3%. ASCE 7-22 wind chapter is not the focus of these design guides and will not be mathematically shown. Instead, only the necessary values and results will be utilized for comparison.

For the new structure, the base shear determined by ASCE 7-22 was 11508 kips with the side wall pressure being -16888 kips (tension). The building natural frequency is 0.129 Hz, and the background and resonant response factors are 0.778 and 1.034, respectively. Note that for this example, the worst-case scenario was considered, meaning that the 240 ft will be used across the wind dimension and will experience the vortex shedding reduction.

For the vortex shedding, following *Figure 4: Vortex Shedding Flowchart Design Guide* the flowchart states in step 2 that the shedding frequency needs to be determined, since the ratio is 2:1 the use of *Figure 2* was needed to determine the Strouhal number. From that, the shedding frequency was as follows:

$$f_s = \frac{0.05\left(212.67\frac{ft}{s}\right)}{240\ ft} = 0.04\ Hz$$

Once the shedding frequency is calculated, step 3 states that since the ratio of the shedding frequency to the building's natural frequency is not 1, the dynamic amplification factor will be utilized in the force reduction.

$$DAF = \frac{1}{\sqrt{(1 - 0.342^2)^2 + \left(2(0.03)(0.342)\right)^2}} = 1.132$$

Step 4 considers the modal projection factor, and since it was not expressed the assumption that the high-rise will act as a cantilever will be used, resulting in a modal factor of 0.39, or the minimum within that range. The last necessary factor will be in step 5 in the form of the peak factor using a 10-minute interval and the shedding frequency from step 2.

$$k_p = \sqrt{2\ln(0.044(600))} + \frac{0.5772}{\sqrt{2\ln(0.044(600))}} = 2.787$$

The last calculation needed will be step 6, combining all factors and calculating the total shedding force along the sidewall at a 10% coherence. Since the structure is a rectangular shape the lift coefficient will be taken as 0.7, resulting in the force being:

$$V_{vortex} = \frac{1}{2}\left(0.0765\frac{lb}{ft^3}\right)\left(212.67\frac{ft}{s}\right)(240ft)(0.7)(640\ ft)^2(0.1)(2.787)(1.132)(0.39)$$

$$= 713\ kips$$

When comparing the vortex shedding to the ASCE 7-22 sidewall force, there is an additional force of 4.22% within this high-rise structure. This again shows that the additional wind effect by vortex shedding can produce noticeable additional sidewall pressure and can increase the total stress load on the frame.

With vortex shedding applied to this structure, the second flowchart, *Figure 5: Dynamic Amplification Flowchart Design Guide,* will be used to see how the base shear differs when considering a moment gust loading factor instead of a code-based approach. The first calculation will be the turbulent intensity based on the exposure classification. Since it was stated that the structure will be considered exposure B the standard roughness length and standard exponent will be 0.98 and 0.22, respectively. This results in a turbulent intensity of:

$$I_H = \frac{1}{\ln\left(\frac{640ft}{0.98\,ft}\right)} = 0.152$$

The next step within the flowchart will be to calculate the moment gust factor using the background and resonant factor from ASCE 7-22. The resonance peak factor (g_r) will be based on 10 minutes and the building's natural frequency.

$$g_r = \sqrt{2\ln(0.129(600))} + \frac{0.5772}{\sqrt{2\ln(0.129(600))}} = 3.15$$

$$G_M = 1 + 2(0.152)\sqrt{3.4^2(0.778) + 3.15^2(1.034)} = 2.35$$

To apply this gust moment factor to the building, the total base bending moment will be determined through step 4. Since the building ratio is now considered a rectangular shape, the drag coefficient will be changed to the new coefficient of 1.5. Once the total base bending moment is calculated, the last step will be to convert that moment into a base shear to be compared to the ASCE 7-22 base shear.

$$M = 2.35(\frac{0.076\frac{lbm}{ft^3}(1.5)(120ft)\left(212.67\frac{ft}{s}\right)^2(640\,ft)^2\left(\frac{1\,lbf}{32.2\frac{lbm\,ft}{s^2}}\right)}{2\big(2+2(0.22)\big)}$$

$$= 3795092.4\ kip - ft$$

$$V = \frac{2(3795092.4\ kip - ft)}{640\ ft} = 11860\ kips$$

Now that the base shear was calculated using MGLF, the comparison can be made to the ASCE 7-22 base shear. The base shear has seen an increase of 3.06%. This shows a contrast to the MGLF applied to the original high-rise case structure. With the square structure, there was a decrease in the overall base shear, but when applied to a rectangular structure, the base shear increased. This shows that the code-based approach from ASCE 7-22 can both overcompensate and undercompensate the base shear depending on the geometry of the structure.

5.2 Conclusion

The additional wind effects not addressed with ASCE 7-22 show that the overall code-based approach can be conservative and overlooks additional effects. The vortex shedding can apply an additional sidewall compression force when compared to ASCE 7-22 base tension sidewall force. While considered small, any additional force along this sidewall can potentially lead to optimization within the moment frame construction. While not expressed in this report, it is recommended that additional research should be conducted on how this additional force can alter the frame sizing and potential changes in construction cost. In addition to the vortex shedding, looking at a moment gust load factor (MGLF) application to the base shear, the ASCE 7-22 both overestimates and underestimates the total shear depending on the geometry of the structure. It should be noted that all calculations and approaches are based on estimated assumptions and references, but should be checked with wind tunnel testing to determine the exact changes along the structure. These findings are not intended to replace code-prescribed wind loads, but rather to inform engineering judgment in cases where additional wind effects influence lateral response. If high-rise design is to be implemented more as time goes on, ASCE 7-22 may want to consider adding sections within the wind chapter that go into more detail regarding these effects, so that ASCE 7 can act as the one reference engineers can turn to for all wind effects rather than looking at multiple different references to limit confusion and errors.

References

American Society of Civil Engineers (ASCE). (2022). *Minimum design loads and associated criteria for buildings and other structures (ASCE/SEI 7-22)*. American Society of Civil Engineers.

Boggs, D., & Dragovich, J. (n.d.). *The nature of wind loads and dynamic response*. In SP-240—Performance-based design of concrete buildings for wind loads. American Concrete Institute.

European Committee for Standardization (CEN). (2005). *Eurocode 1: Actions on structures—Part 1-4: General actions—Wind actions (EN 1991-1-4)*. CEN.

Daemei, A. B., Darvish, A., Aeinehvand, R., & Razzaghipour, A. (2021). Large-eddy simulation (LES) on the square and triangular tall buildings to measure drag force. *Advances in Civil Engineering*, 2021, Article 6666895.

Htun, T. (2016). A simplified approach on dynamic response of tall buildings due to wind loads. *International Journal for Innovative Research in Multidisciplinary Field*, 2(9).

International Code Council (ICC). (2021). *International building code*. International Code Council.

Kareem, A., & Zhou, Y. (2003). Gust loading factor—Past, present and future. *Journal of Wind Engineering and Industrial Aerodynamics*, 91, 1301–1328.

Li, J., Hong, G., & Xu, H. (2024). Wind load effects and gust loading factor for cable-suspended photovoltaic structures. *Energies*, 17(38).

Liu, Y., Kopp, G. A., & Chen, S. (2021). An examination of the gust effect factor for rigid high-rise buildings. *Frontiers in Built Environment*, 7.

Lopatinski, V. (2020). *Vortex induced vibrations in high-rise buildings* (Master's thesis). Aalto University.

Torkamani, M. A. M., & Pramono, E. (1985). Dynamic response of tall building to wind excitation. *Journal of Structural Engineering*, 111(4), 805–825.

WorldAtlas. (2025, November 8). *US cities with the most skyscrapers*. https://www.worldatlas.com/cities/us-cities-with-the-most-skyscrapers.html

Zhou, Y., & Kareem, A. (2001). Gust loading factor: New model. *Journal of Structural Engineering*, 127(2), 168–175